

Modeling the sensitivity of shaped DAS fibre-optic cables to elastic wave data

Matt Eaid and Kris Innanen
University of Calgary - CREWES

Summary

The interest in Distributed Acoustic Sensing (DAS) fibres, for improved Geophysical acquisition has seen substantial growth over the last half-decade. Utilizing DAS fibre for seismic acquisition has the potential to decrease acquisition costs, improve survey repeatability, and expand the applications of seismic acquisition. Straight DAS fibres have obtained a certain degree of success, however, their insensitivity to wavefields producing broadside strain has greatly limited their applications. Fibre geometry plays a crucial role in the ability of DAS systems to recover the wavefield, and winding the fibre in more complex shapes, has proven to better characterize the wavefield. Unfortunately, as the complexity of the fibre geometry grows, so does the complexity of the recorded signal, making interpretation a more challenging task. To develop a more thorough appraisal of DAS fibre shapes, we must be able to model the response of varying fibre geometries to an impinging wavefield. We begin with a review of the main tenants of the fibre geometry model, which make up the core of the CREWES fibre geometry and sensing model (FGSM). We then couple this with a velocity-stress finite-difference model, and show how it may be utilized to create synthetic fibre data.

Introduction

For decades, the standard geophone has been the instrument of choice for the measurement of seismic wavefields. Current economic pressures coupled with a change in the role of seismic acquisition has driven a need for innovative and cost-effective seismic acquisition technologies. Distrusted Acoustic Sensing (DAS) which utilizes standard telecommunication grade fibre-optics to sense seismic motion has significantly increased in popularity in recent years. The recent expansion of fibre-optics into the telecommunications industry has reduced the cost of optical fibres, making them an attractive option for seismic acquisition programs.

Optical fibres contain microscopic impurities that act as sites for Rayleigh scattering within the fibre. As a laser pulse traverses the fibre, it interacts with these impurities, and a portion of the light is backscattered. This backscattered light arrives at what is known as the interrogator, where its intensity and pattern are analyzed. When a fibre is subjected to seismic strain it is stretched and squeezed along the tangent of the fibre. This stretching and squeezing changes the distance between scattering impurities, altering the optical path length of the laser pulse, which further alters the intensity of the backscattered light. The interrogator uses the change in light intensity over time to interpret a seismic signal, and produce shot records.

Recent publications have exemplified the vast applications that DAS could be applied to. Daley et al. (2013), Mateeva et al. (2014), and Mestayer et al. (2012) examined the use of straight DAS fibres for vertical seismic profiles. Webster et al. (2016) employed straight DAS fibres in deviated wells to detect microseismic events during fracking. Martin et al. (2017) examined the use of DAS arrays for passive monitoring of teleseismic waves and anthropogenic noise. Research at the University of Calgary has examined the discrimination of elastic wave modes through the shape of DAS fibres (Innanen and Eaid, 2017), and the characterization of microseismic source mechanisms (Innanen et al., 2017). It is also hoped

GeoConvention 2018

that properties of DAS acquisition could aid in issues encountered in FWI, namely frequency content and spatial sampling. For these research areas to be fully realized, and as fibre geometry increases in complexity, it is imperative to develop tools to model the response of DAS fibres to seismic wavefields. The CREWES fibre geometry and sensing model (FGSM) has been in development for the last year, it is concerned with the geometry of the fibre, and can handle input snapshots of a wavefield. We expand upon this by developing a velocity-stress finite-difference formulation that is appropriate for DAS data, and then couple it to the geometric model in the FGSM to produce synthetic fibre data.

Geometrical model for a helically wound fibre

We begin by imagining a DAS fibre wrapped in a helix, around a cable of arbitrary shape.

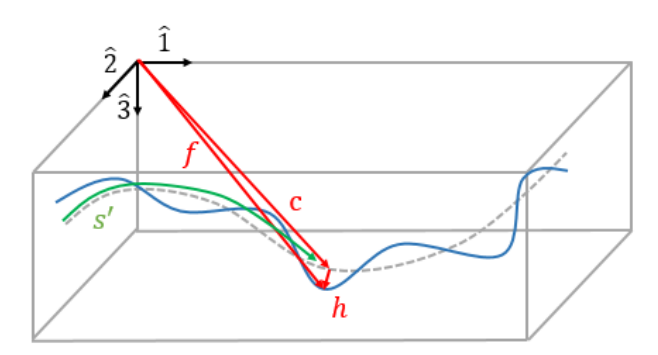


Figure 1: Schematic showing the fibre position \mathbf{f} , constructed from a sum of the cable position \mathbf{c} , and the helix position \mathbf{h} . Along with the arc length along the fibre.

Position vector, \mathbf{f} , represents the position of any point on the fibre, which may be decomposed into the vector sum of the vectors \mathbf{c} , and \mathbf{h} . Where vector \mathbf{c} is the position of the point on the central axis of the cable closest to point \mathbf{f} , and vector \mathbf{h} is vector lying in the plane perpendicular to the cable axis that adds in a helix as the cable winds. Typically the cable position is parameterized in the arc-length along the cable, \mathbf{s}' , taking the form, $\mathbf{c} = [c_1(\mathbf{s}'), c_2(\mathbf{s}'), c_3(\mathbf{s}')]^T$. Where cable arc-length is given by,

$$\mathbf{s}'(x) = \int_0^x dx' \left[\left(\frac{dc}{dx'} \right) \cdot \left(\frac{dc}{dx'} \right) \right]^{1/2} \tag{1}$$

We may then a define new coordinate system defined by the cable axis tangent, $\hat{\boldsymbol{t}}(s')$, and the two vectors lying in the plane perpendicular to the tangent, the normal, $\hat{\boldsymbol{n}}(s')$, and binormal, $\hat{\boldsymbol{b}}(s')$.

$$\hat{\boldsymbol{t}}(s') = \frac{dc}{ds'}, \ \boldsymbol{n}(s') = \frac{d\boldsymbol{t}(s')}{ds'}, \ \hat{\boldsymbol{b}}(s') = \hat{\boldsymbol{t}}(s') \times \hat{\boldsymbol{n}}(s')$$
 (2)

In the tangent, normal, binormal coordinate system, for the special case of a straight cable, with a helically wound cable,

$$f = c + h = \begin{bmatrix} s' \\ r\cos(s'/v) \\ r\sin(s'/v) \end{bmatrix} = \begin{bmatrix} s' \\ 0 \\ 0 \end{bmatrix} + \begin{bmatrix} 0 \\ r\cos(s'/v) \\ r\sin(s'/v) \end{bmatrix}$$
(3)

With $v(\gamma) = r \tan(\gamma)$. If we instead have an arbitrary cable, and we rotate the helix into the standard cartesian system.

$$\begin{bmatrix} f_1(s') \\ f_2(s') \\ f_3(s') \end{bmatrix} = \begin{bmatrix} c_1(s') \\ c_2(s') \\ c_3(s') \end{bmatrix} + R(s') \begin{bmatrix} 0 \\ r\cos(s'/v) \\ r\sin(s'/v) \end{bmatrix}$$
(4)

Where, \mathbf{R} , is the rotation matrix, taking the helix from the tangent, normal, and binormal coordinate system to the classic Cartesian system. The final and most important quantity required of the FGSM geometric model is the fibre tangent, $\widehat{T} = df/ds$. It is along this tangent direction that the interrogator senses seismic strain.

Velocity-stress finite-difference formulation

Finite-difference schemes based on a velocity-stress formulation rely on the computation of particle velocity, and stress to propagate a wavefield by solving the elastodynamic equation of motion (i), Hooke's law (ii), and the stress-strain relation (iii):

i.
$$\rho \frac{\partial^2 u_i}{\partial t^2} = \nabla \cdot \sigma + f_i$$
 ii. $\sigma_{ij} = c_{ijkl} e_{kl}$ iii. $e_{kl} = \frac{1}{2} \left(\frac{\partial u_k}{\partial x_l} + \frac{\partial u_l}{\partial x_k} \right)$ (5)

Taking the time derivative of the stress-strain relation, and substituting particle velocity for the derivative of the displacement with respect to time, the velocity-stress finite-difference scheme solves for the particle velocity and stress at each time step. Doing so on a grid where stress and velocity are staggered from each other by a half time step, and where each component of velocity (stress) is offset by a half step in space is the most stable scheme. Solving equations 5 (i) and (ii), in an alternating fashion produces snapshots of the wavefield at each time. Remembering that DAS fibres measure the tangential strain along the fibre, we require a measurement of strain from our finite-difference model. Recognizing that the time derivative of the stress strain relation relies solely on spatial derivatives of the particle velocity, we may readily compute the strain rate (e_{kl}) from values computed during the wave propagation.

$$\begin{bmatrix} e_{tt}^{\cdot} & e_{tn}^{\cdot} & e_{tb}^{\cdot} \\ e_{nt}^{\cdot} & e_{nn}^{\cdot} & e_{nb}^{\cdot} \\ e_{bt}^{\cdot} & e_{bn}^{\cdot} & e_{bb}^{\cdot} \end{bmatrix} = R \begin{bmatrix} 2\dot{u}_{x,x} & \dot{u}_{x,y} + \dot{u}_{y,x} & \dot{u}_{x,z} + \dot{u}_{z,x} \\ \dot{u}_{y,x} + \dot{u}_{x,y} & 2\dot{u}_{y,y} & \dot{u}_{y,z} + \dot{u}_{z,y} \\ \dot{u}_{z,x} + \dot{u}_{x,z} & \dot{u}_{z,y} + \dot{u}_{y,z} & 2\dot{u}_{z,z} \end{bmatrix} R^{T}$$
(6)

Rotating the strain rate tensor back into the tangent, normal, and binormal coordinate system, and extracting the tangential (\dot{e}_{tt}) component at every spatial location, gives the response of DAS fibre to the progating wavefield at a given time. Repeating this for every time step in the finite difference simulation gives the resulting shot record for the DAS fibre geometry of the FGSM.

Examples

Computing the response of a 1C geophone to a wavefield, using the velocity-stress method can be achieved simply by extracting the value of the particle velocity at the geophone locations at each time step. Conversely, when computing the response of a DAS fibre, the situation becomes more complex. The six strain rate components, an example of which are shown in figure 2 must be computed, rotated into the tangent, normal, and binormal coordinate system, and the tangential component must be extracted at each timestep. Figures 3,4, and 5 show the modeled response of straight, helical wound, and nested two-helix respectively. Figure 3, shows the well-known broadside insensitivity of straight DAS fibres, where the fibre is least sensitive to wave impinging at near normal angles. Figures 4 and 5 show that more complex fibre geometries remedy this problem, but that the resulting signal is more complex.

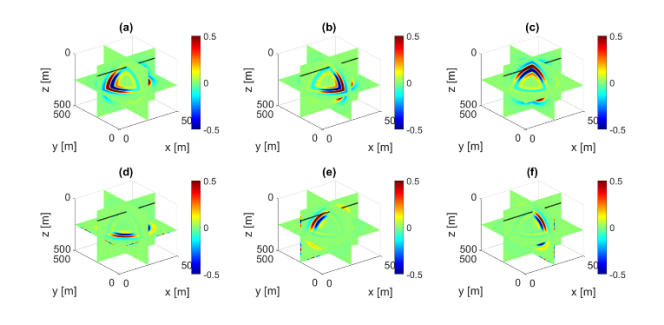


Figure 2: Strain rate tensors: (a) \dot{e}_{xx} , (b) \dot{e}_{yy} , (c) \dot{e}_{zz} , (d) \dot{e}_{xy} , (e) \dot{e}_{xz} , (f) \dot{e}_{yz}

Figure 3: Response of a straight fibre to a wavefield

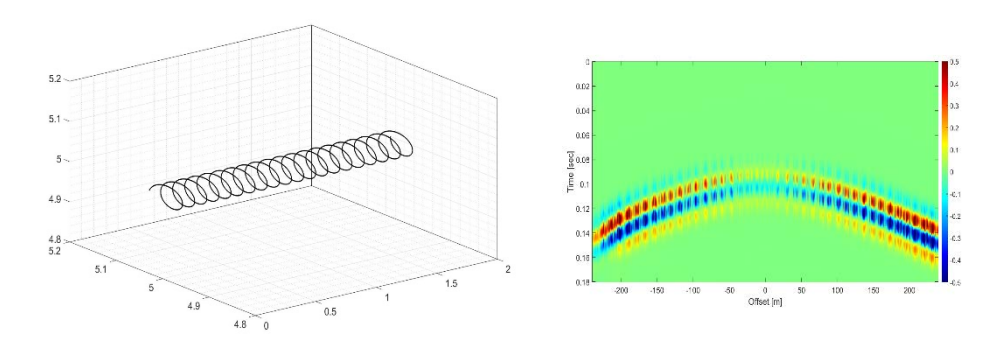


Figure 4: An example of a helically wound fibre (left), and the resulting shot record (right).

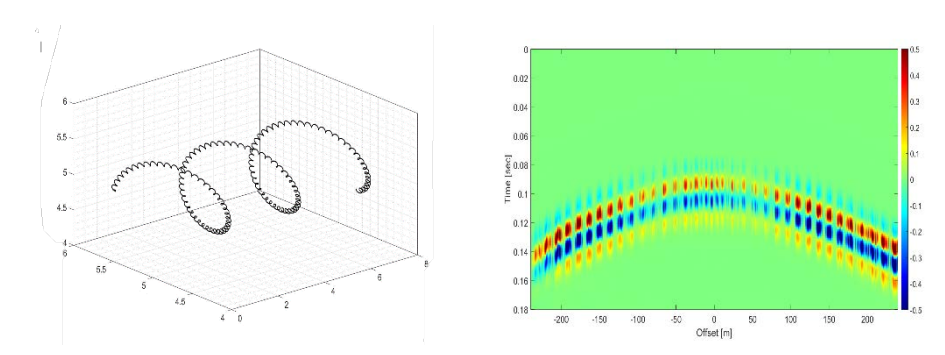


Figure 5: An example of a nested two-helix fibre (left), and the resulting shot record (right).

Conclusions

We briefly build review the CREWES fibre geometry and sensing model and add to it by developing tools that allow for the creation of shot records from a propagating wavefield. This tool will allow for the appraisal and laboratory testing of candidate fibre geometry shapes, with the goal of being able to design fibres with shapes that suppress portions of the wavefield. Additionally, any inverse problem that hopes to use DAS data, will require a forward model, a tool which we have now developed. It is hoped that this work will find use in applications to FWI and microseismic source evaluation.

Acknowledgements

The authors would like to thank CREWES industrial sponsors, the SEG, and NSERC under the grant CRDPJ 461179-13 for funding this work and making it possible.

References

Daley, T., Freifeld, B., Ajo-Franklin, J., Dou, S., Pevzner, R., Shulakova, V., Kashikar, S., Miller, D., Goetz, J., Henninges, J., and Lueth, S., 2013, Field testing of fibre-optic Distributed Acoustic Sensing (DAS) for subsurface seismic monitoring.: The Leading Edge

Innanen, K., Eaid., M., 2017, Design of DAS fibres for elastic wave mode discrimination, CREWES Research Reports, No. 35

Innanen, K., Mahmoudian, F., Eaid, M., 2017, Detection and characterization of microseismic sources with shaped DAS fibre, CREWES Research Reports, No. 38

Martin, E., Biondi, B., Cole, S., and Karrenbach, M., 2017, Continuous subsurface monitoring by passive seismic data recorded with Distributed Acoustic Sensors: the "Stanford DAS Array" experiment.: EAGE Expanded Abstracts.

Mateeva, A., Lopez, J., Potters, H., Mestayer, J., Cox, B., Kiyashchenko, D., Wills, P., Grandi, S., Hornman, K., Kuvshinov, B., Berlang, W., Yang, Z., and Detomo, R., 2014, Distributed Acoustic Sensing for reservoir monitoring with vertical seismic profiling.: Geophysical Prospecting, 62.

Mestayer, J., Karam, S., Cox, B., Wills, P., Mateeva, A., Lopez, J., Hill, D., and Lewis, A., 2012, Distributed Acoustic Sensing for geophysical monitoring.: EAGE Expanded Abstracts.

Webster, P., Molenaar, M., and Perkins, C., 2016, DAS microseismic: CSEG Recorder Focus Article, 38-39